

## A STUDY OF THE EFFECTS OF JUPITER IN SPACE TRAJECTORIES

**Antonio Fernando Bertachini de Almeida Prado**

Instituto Nacional de Pesquisas Espaciais – São José dos Campos-SP-12227-010

Phone (012) 345-6201 – Fax (012) 3456226 – E-mail: [prado@dem.inpe.br](mailto:prado@dem.inpe.br)

**Roger A. Broucke**

Department of Aerospace Eng. and Eng. Mechanics, University of Texas at Austin.

### ABSTRACT

In the present paper we study and classify the Swing-by maneuvers that use the planet Jupiter as the body for the close approach. The goal is to simulate a large variety of initial conditions for those orbits and classify them according to the effects caused by the close approach with Jupiter in the orbit of the spacecraft. The well-known planar restricted circular three-body problem is used as the mathematical model. The equations are regularized (using Lemaître's regularization), so it is possible to avoid the numerical problems that come from the close approach with Jupiter. After that, the velocity increment required to start or to stop the spacecraft at the Earth and the flight path angle at the meeting point are calculated. A section is also written to compare the results obtained with the dynamics given by the restricted problem and the “patched-conics” approximation.

**Key Words:** Astrodynamics, Restricted Problem, Swing-By, Space Trajectories.

### INTRODUCTION

The Swing-By maneuver is a technique used in several missions to reduce fuel consumption like in Weinstein, 1992; Swenson, 1992; Farquhar and Dunham, 1981; Minovich, 1961; Dowling et. al., 1991; Flandro, 1966; Farquhar et. al. 1985; Dunham and Davis, 1985; Prado, 1996, 1997 and 1999; Prado and Broucke, 1995a and 1995b; Broucke and Prado, 1993.

Among the several sets of initial conditions that can be used to identify uniquely one trajectory, the same one used in the paper written by Broucke (1988) is used here. It is composed by the following variables: 1)  $J$ , the Jacobian constant of the spacecraft (an integral of the restricted three-body problem); 2) The angle  $\mathbf{y}$ , that is defined as the angle between the line  $M_1$ - $M_2$  (Sun-Jupiter) and the direction of the periapsis of the trajectory of the spacecraft around Jupiter; 3)  $R_p$ , the distance from the spacecraft to the center of Jupiter in the moment of the closest approach with Jupiter (periapsis distance). Note that the Jacobian constant is essentially equivalent to the velocity at periapsis or the hyperbolic excess velocity  $V_\infty$ , since they can be related by one single expression.

For a large number of values of these three variables, the equations of motion are integrated numerically forward and backward in time, until the spacecraft is at a

distance that can be considered far enough from Jupiter, such that the Jupiter's effect is neglected and the system formed by the Sun and the spacecraft can be considered a two-body system. At these two points, two-body celestial mechanics formulas are valid for the computation of the energy and the angular momentum before and after the close approach. Those quantities are used to identify up to sixteen classes of orbits, according to the changes in the energy and angular momentum caused by the close encounter.

It is especially checked which ones of those orbits have a passage near the Earth in the outbound (starting at the Earth) and in the inbound (starting at Jupiter) trajectories. This is very important, because only those orbits have a potential for practical application in transfers from/to the Earth. The results are shown in letter-plots, where one letter describing the effects of the Swing-by is plotted in a two-dimensional graph that has in the horizontal axis the angle  $\gamma$  (the angle between the periapsis vector and the Sun-Jupiter line) and in the vertical axis the Jacobian constant of the spacecraft. There is one plot for each value of the parameter  $R_p$ . After that, the velocity change required to start or to stop the spacecraft at the Earth and the flight path angle at the meeting point are calculated. This paper has to be considered as a continuation of Broucke (1988); Prado and Broucke (1993) and Prado (1999).

### DEFINITION OF THE PROBLEM

To solve the problem described above, it is assumed the existence of three bodies: the Sun, the planet Jupiter and a third particle of negligible mass (the spacecraft). It is also assumed that the total system (Sun + Jupiter + spacecraft) satisfies the hypothesis of the planar restricted circular three-body problem: all the bodies are point masses; the Sun and Jupiter are in circular orbits around their mutual center of mass.

With these assumptions, the problem consists in studying the motion of the spacecraft near the close encounter with the planet Jupiter. In particular, the energy and the angular momentum of the spacecraft before and after this close encounter are calculated, to detect the changes in the trajectory during the close approach. The orbits are classified in four categories: elliptic direct (negative energy and positive angular momentum), elliptic retrograde (negative energy and angular momentum), hyperbolic direct (positive energy and angular momentum) and hyperbolic retrograde (positive energy and negative angular momentum). The problem now is to identify the category of the orbit of the spacecraft before and after the close encounter with Jupiter. Fig. 1 explains the geometry involved in the close encounter.

The spacecraft leaves the point A, crosses the horizontal axis (the line between the Sun and the planet Jupiter), passes by the point P (the periapsis of the trajectory of the spacecraft around Jupiter) and goes to the point B. Points A and B are chosen in a such way that the influence of Jupiter at those points are neglected and, consequently, the energy is constant after B and before A. Two of the initial conditions are clearly identified in this figure: the periapsis distance  $R_p$  (distance measured between the point P and the center of Jupiter) and the angle  $\gamma$ , measured from the horizontal axis in the counter-clock-wise direction. The distance  $R_p$  is not to scale, to make the figure easier to understand. The third initial condition is the Jacobian constant  $J$  of the spacecraft. The second part of the problem is to identify if one particular trajectory passes near the Earth in one or in both directions of time. For that purpose, the numerical integration is extended in each direction of time until one of the following events occur: i) The spacecraft reaches a position inside the Earth's orbit around the Sun. Then it is assumed that the spacecraft crosses the Earth's path in space and, with proper timing conditions, a close encounter with the Earth is possible; ii) The spacecraft goes to far from the Solar

System without crossing the Earth's path. Then it is assumed that it does not come back again and a close encounter with the Earth is not possible; iii) The spacecraft remains close to the Solar System, but too much time has been passed without a crossing with the Earth's path. Then it is assumed that a useful close encounter with the Earth is not likely to occur.

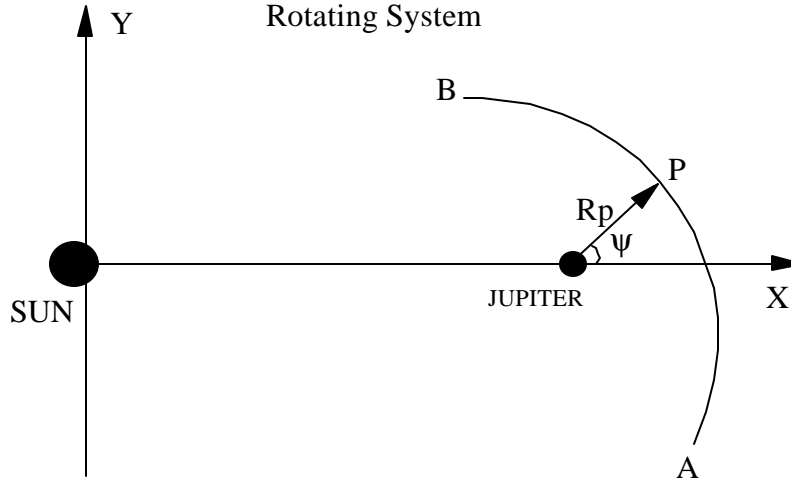


Fig. 1 - Geometry of the Close Encounter

### MATHEMATICAL MODEL AND ALGORITHM

The equations of motion for the spacecraft are assumed to be the ones valid for the well-known planar restricted circular three-body problem:

$$\ddot{x} - 2\dot{y} = x - \frac{\partial V}{\partial x} = \frac{\partial W}{\partial x} \quad \ddot{y} + 2\dot{x} = y - \frac{\partial V}{\partial y} = \frac{\partial W}{\partial y} \quad (1-2)$$

$$W = \frac{1}{2}(x^2 + y^2) + \frac{(1-m)}{r_1} + \frac{m}{r_2} \quad (3)$$

The usual standard canonical system of units is used. It is also necessary to have equations to calculate the energy and the angular momentum of the spacecraft. It can be done with the formulas:

$$E = \frac{(x + \dot{y})^2 + (\dot{x} - y)^2}{2} - \frac{1-m}{r_1} + \frac{m}{r_2}, \quad C = x^2 + y^2 + x\dot{y} - y\dot{x} \quad (4-5)$$

With those equations, it is possible build a numerical algorithm to solve the problem. It has the following steps:

- i) Arbitrary values for the three parameters:  $R_p$ ,  $J$ ,  $\mathbf{y}$  are given;

ii) With these values the initial conditions in the rotating system are computed. The initial position is  $X_i = R_p \cos(\mathbf{y}) + (1 - \mathbf{m})$ ,  $Y_i = R_p \sin(\mathbf{y})$  and the initial velocity is  $V_{Xi} = -V \sin(\mathbf{y})$ ,  $V_{Yi} = +V \cos(\mathbf{y})$ , where  $V = \sqrt{\dot{x}^2 + \dot{y}^2}$ ;

iii) With these initial conditions, the equations of motion are integrated forward in time until the distance between the planet Jupiter and the spacecraft is bigger than a specified distance limit  $d_{JS}$ . At this point the numerical integration is stopped and the energy ( $E_+$ ) and the angular momentum ( $C_+$ ) after the encounter with Jupiter are calculated;

iv) Then the initial conditions are returned to the point P, and the equations of motion are integrated backward in time, until the distance  $d_{JS}$  is reached again. Then the energy ( $E_-$ ) and the angular momentum ( $C_-$ ) before the encounter with Jupiter are obtained;

v) With those results, all the information required to calculate the change in energy ( $E_+ - E_-$ ) and angular momentum ( $C_+ - C_-$ ) due to the close approach with Jupiter are available;

vi) Now, the numerical integration is extended beyond the points A and B and it is verified if the spacecraft has none, one or two possible close encounters with the Earth, by using the conditions described in the previous section;

With this algorithm available, the given initial conditions (values for  $R_p$ ,  $J$  and  $\mathbf{y}$ ) can be varied in any desired range to study the effects of the close approach with Jupiter in the orbit of the spacecraft.

## RESULTS

The results consist of plots that show the change of the orbit of the spacecraft due to the close encounter with the planet Jupiter, for a large range of given initial conditions. First of all it is necessary to classify all the close encounters between Jupiter and the spacecraft, according to the change obtained in the orbit of the spacecraft. The letters A to P are used for this classification, according to the rules showed in Table 1.

**Table 1** - Rules for the assignment of letters to orbits

Before:	After:	Direct Ellipse	Retrograde Ellipse	Direct Hyperbola	Retrograde Hyperbola
Direct Ellipse		A	E	I	M
Retrograde Ellipse		B	F	J	N
Direct Hyperbola		C	G	K	O
Retrog. Hyperbola		D	H	L	P

To indicate which ones of those orbits have possibility of one or two close encounters with the Earth, the following conventions are used: i) Letters in capital case for orbits that do not cross the Earth's path around the Sun and have no possibility of a close encounter with the Earth; ii) Letters in lower case for orbits that cross the Earth's path around the Sun in only one direction of time. These orbits can be used to send a spacecraft from the Earth to the Jupiter or somewhere else using a Swing-by in Jupiter; iii) Letters in bold lower case for orbits that cross the Earth's path around the Sun in both directions of time. These orbits can be used to send a spacecraft from the Earth to the Jupiter; from Jupiter to the Earth; or from the Earth to the Jupiter and back to the Earth, without additional maneuvers, if a proper timing condition can be found.

With those rules defined, the results consist of assigning one of those letters to a position in a two-dimensional diagram that has the parameter  $\mathbf{y}$  in the horizontal axis and the parameter  $J$  in the vertical axis. There is one plot for each desired value of the periapsis distance. The range for the variables used here is  $\mathbf{y}$  ( $180^\circ \leq \mathbf{y} \leq 360^\circ$ ) and  $J$  ( $-1.35 \leq J \leq 1.55$ ). They are very adequate in showing the main characteristic of the plots. The interval  $180^\circ \leq \mathbf{y} \leq 360^\circ$  is used, and not the full range ( $0^\circ \leq \mathbf{y} \leq 360^\circ$ ), because there is a symmetry between the chosen interval and the complementary interval  $0^\circ \leq \mathbf{y} \leq 180^\circ$ . This symmetry comes from the fact that an orbit with an angle  $\mathbf{y} = \mathbf{q}$  is different from an orbit with an angle  $\mathbf{y} = \mathbf{q} + 180^\circ$  only by a time reversal. It means that there is a correspondence between these two intervals. This correspondence is:  $I \leftrightarrow C$ ,  $J \leftrightarrow G$ ,  $L \leftrightarrow O$ ,  $B \leftrightarrow E$ ,  $N \leftrightarrow H$ ,  $M \leftrightarrow D$ . The orbits A, F, K and P are unchanged.

To decide the best range of values for the third parameter (periapsis distance) several exploratory simulations have to be made. It was noticed that, for values greater than 50 Jupiter's radius, the effects of the Swing-by are very small, with the exception of very few special cases. Then, it is decided to make plots for the values: 1.1, 1.5, 2.0, 5.0, 10.0 and 50.0 Jupiter's radius. They span a useful range of values and they are able to show very well the evolution of the effects. Fig. 2 shows a series of diagrams covering the desired range for all the three variables.

To have a better understanding of the process, some of the trajectories are plotted in the rotating and fixed frame in Fig. 3. The orbits of type N, j and **b** are chosen as examples. Table 2 gives some of the numerical data for those trajectories, including the initial conditions. The numerical values for the limits involved in the results available in this research (in canonical units) are: Distance from Jupiter to the points A and B ( $d_{JS}$ ): 0.5; Distance limit for the spacecraft to be considered too far from the Solar System: 2.0; Time limit to stop the numerical integration when searching for a passage close to the Earth: 10.0. Trajectories j and **b** cross the Earth's orbit making an angle close to 90 degrees, so they are not very useful for practical applications due to the high increment velocity required by the maneuver. They have to be considered just as examples of the trajectories available. The results of this paper makes a survey of a large range of trajectories, including the ones with the lowest possible increments of velocity and flight path angle close to zero.

The trajectories that have only one encounter with the Earth are studied in more detail, to see if they encounter the Earth before or after the Swing-by with Jupiter. The curious result is that only trajectories that encounter with the Earth before the Swing-by with Jupiter are found. It means that the only type of trajectory that encounter the Earth after the Swing-by found in this research is the one that has a double-crossing (before and after the Swing-by) with the Earth's path around the Sun.

Fig. 4 shows the variation in energy obtained using the restricted problem model for the case  $R_p = 1.1 R_j$ . It is clear the symmetry around the line of angle of approach  $180^\circ$ .

### THE EXCESS VELOCITIES AND THE FLIGHT PATH ANGLE

After finding all those orbits, it is interesting to know the magnitudes of the impulses ( $DV$ ) required to start the outbound trajectories at the Earth (to go to Jupiter), or to stop the inbound trajectories at the Earth (coming from Jupiter). It is assumed that the impulse required is the difference between the inertial velocities of the Earth and the spacecraft. It means that the spacecraft is assumed to be traveling attached to the Earth (they both have the same position and velocity at a given time), but it is free of the attraction of the Earth's gravity field. In other words, the impulse required to escape the Earth is not included in the results shown here. Another quantity calculated is the flight

path angle at the Earth, which is defined as the angle between the inertial velocities of the spacecraft and the Earth at the point that their orbits intersect. Figs. 5 to 7 show the results. All the plots have the angle of approach  $\psi$  (in degrees) in the horizontal axis and the Jacobian Constant in the vertical axis. They are: i) The flight path angle (in degrees) for the outbound trajectories; ii) The outcoming excess velocity (in canonical units) to start the outbound trajectories; iii) The flight path angle (in degrees) for the inbound trajectories; iv) The incoming excess velocity (in canonical units) to stop the inbound trajectories; v) The addition of the two excess velocities, also in canonical units. From those figures it is easy to find the regions with minimum excess velocities. It corresponds, as expected, to the regions with flight path angle close to zero.

**Table 2** - Numerical data for the trajectories plotted in Fig. 3

Orbit	$J$	$R_p$	$\psi$	$E_-$	$E_+$	$DE$	$C_-$	$C_+$	$DC$
N	0.70	$10R_J$	216	-0.2021	0.2706	0.4727	-0.9021	-0.4294	0.4727
j	0.00	$10R_J$	237	-0.2872	0.4631	0.7503	-0.2872	0.4631	0.7503
b	-0.85	$10R_J$	192	-0.9573	-0.7450	0.2123	-0.1073	0.1050	0.2123

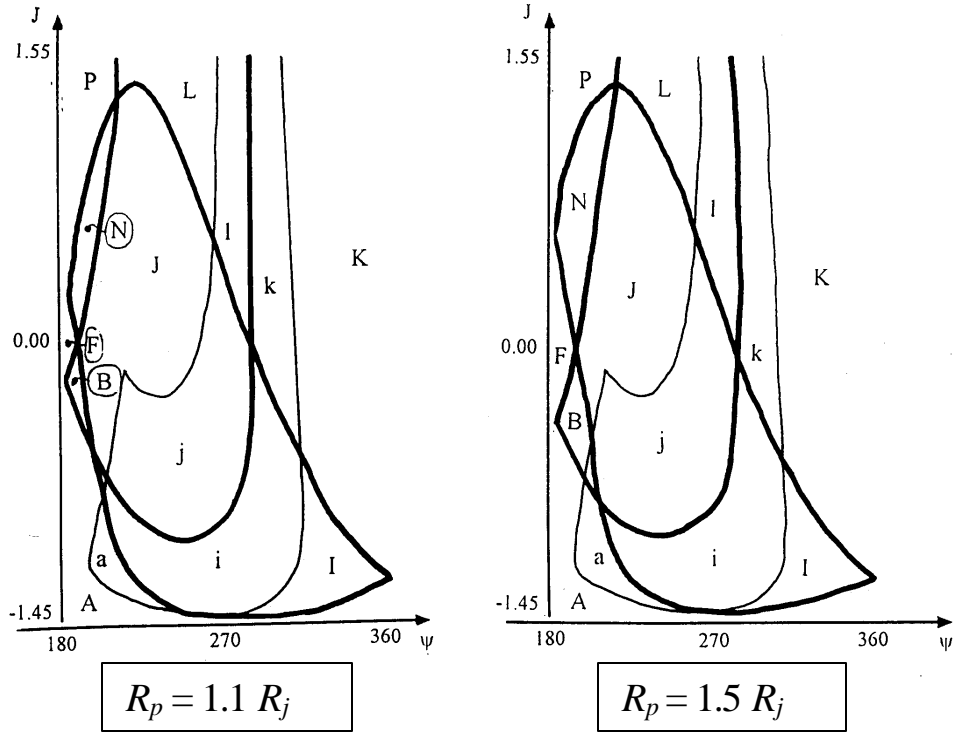
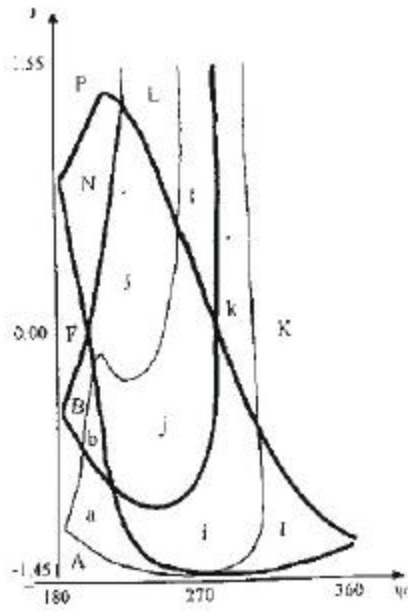
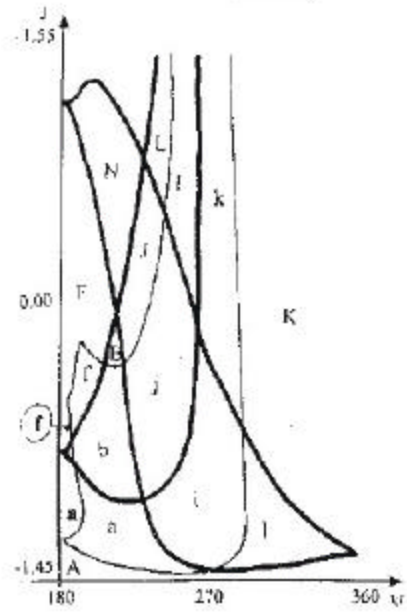


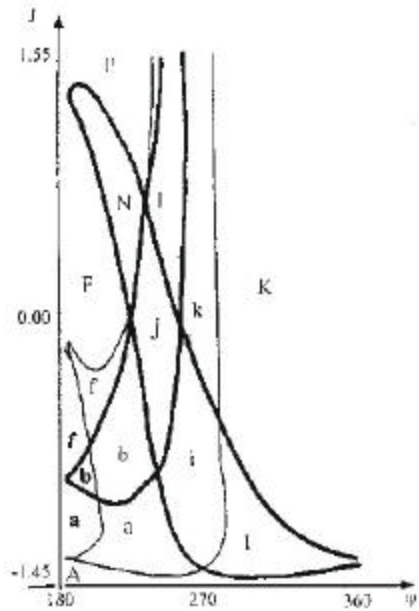
Fig. 2 - Results for  $R_p = 1.1, 1.5, 2.0, 5.0, 10.0, 50.0$ .



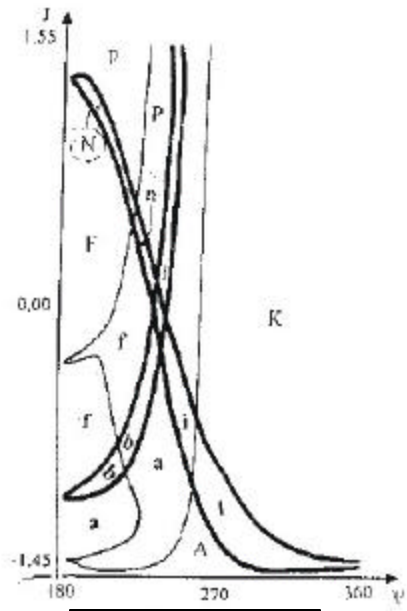
$$R_p = 2.0 R_j$$



$$R_p = 5.0 R_j$$



$$R_p = 10.0 R_j$$



$$R_p = 50.0 R_j$$

Fig. 2 (Cont.) - Results for  $R_p = 1.1, 1.5, 2.0, 5.0, 10.0, 50.0$ .

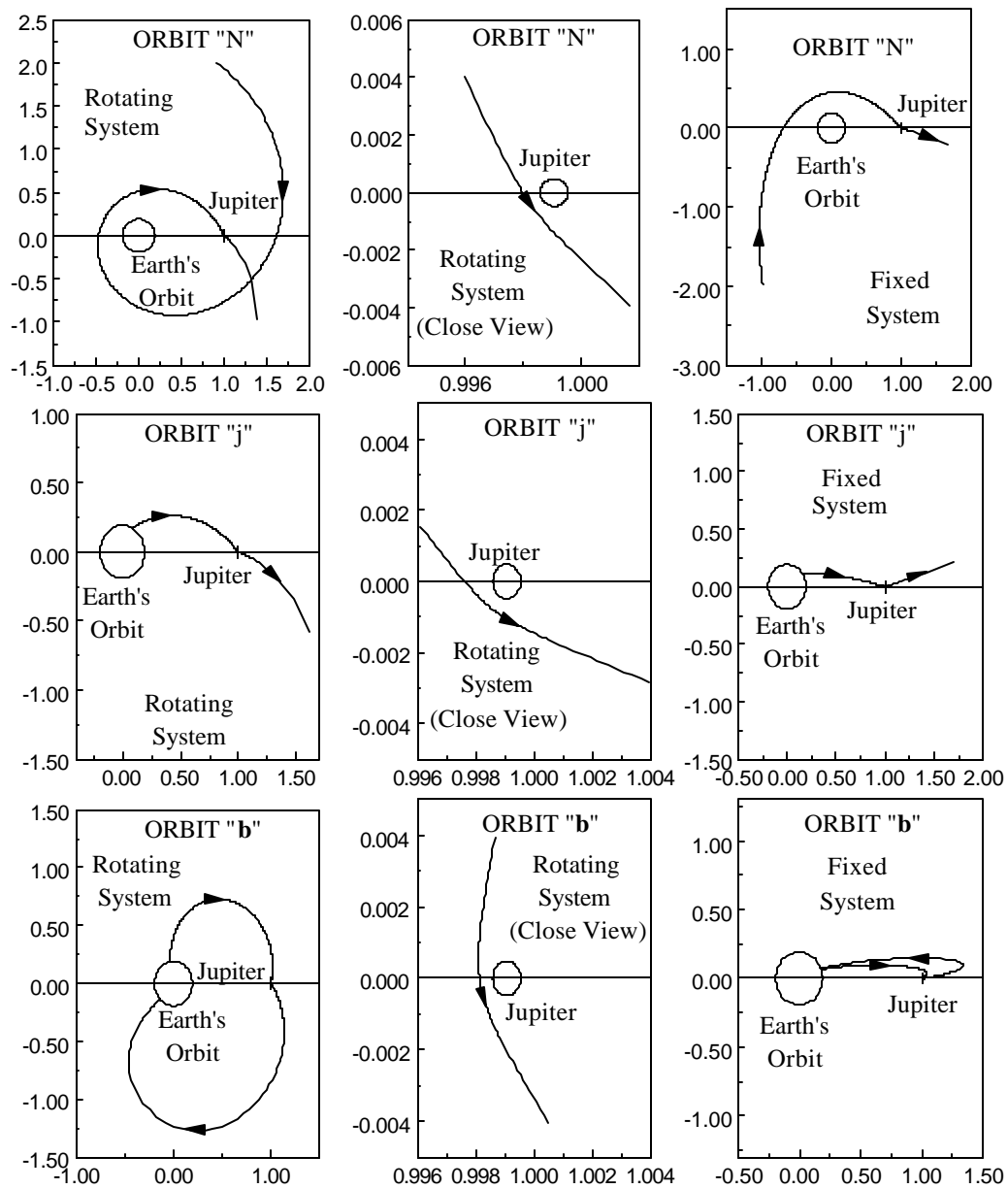


Fig. 3 - Examples of Trajectories in the Rotating and Fixed Reference Frame.



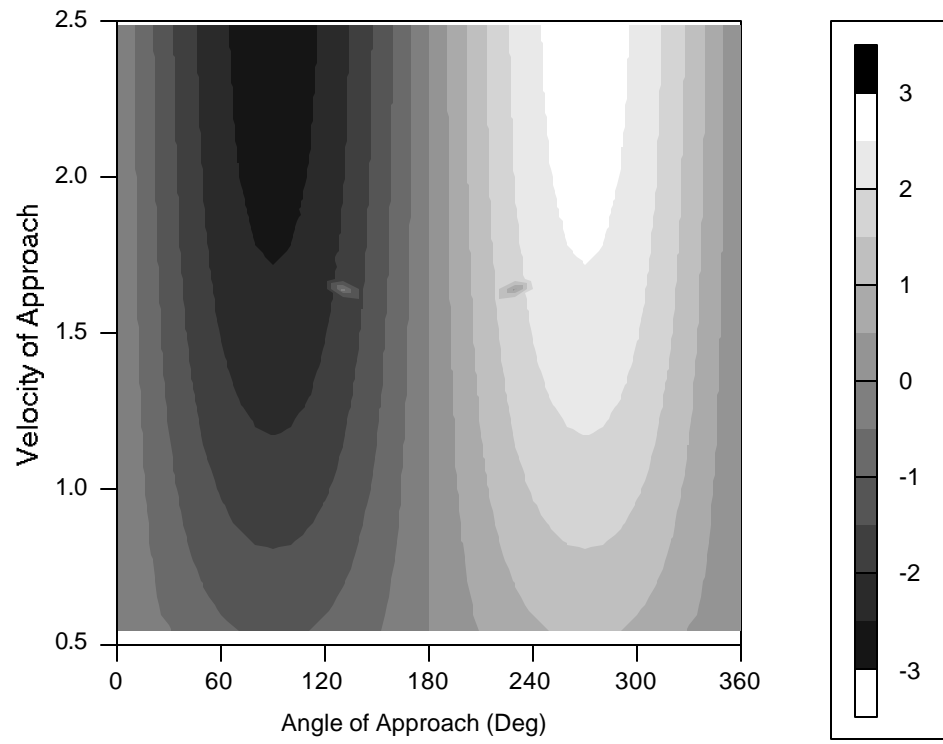


Fig. 4– Variation in Energy Using the Restricted Problem Model for  $R_p = 1.1 R_j$ .

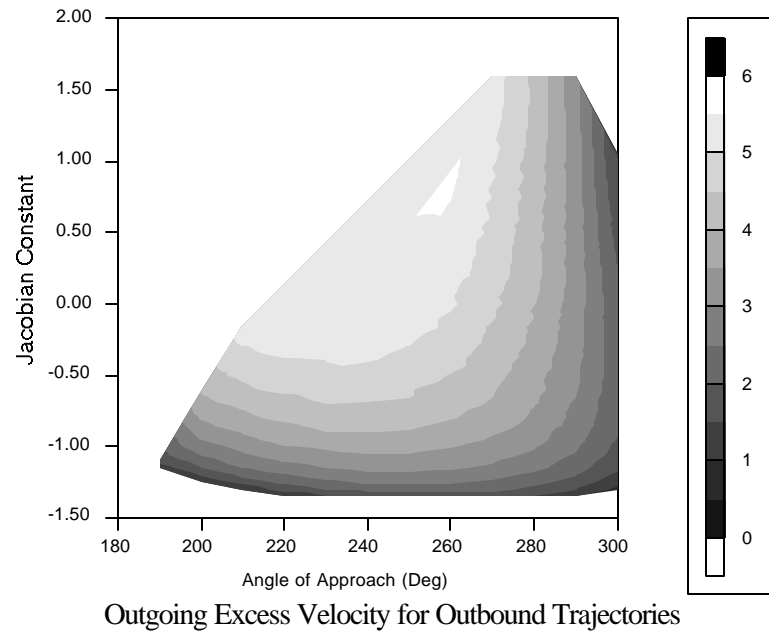
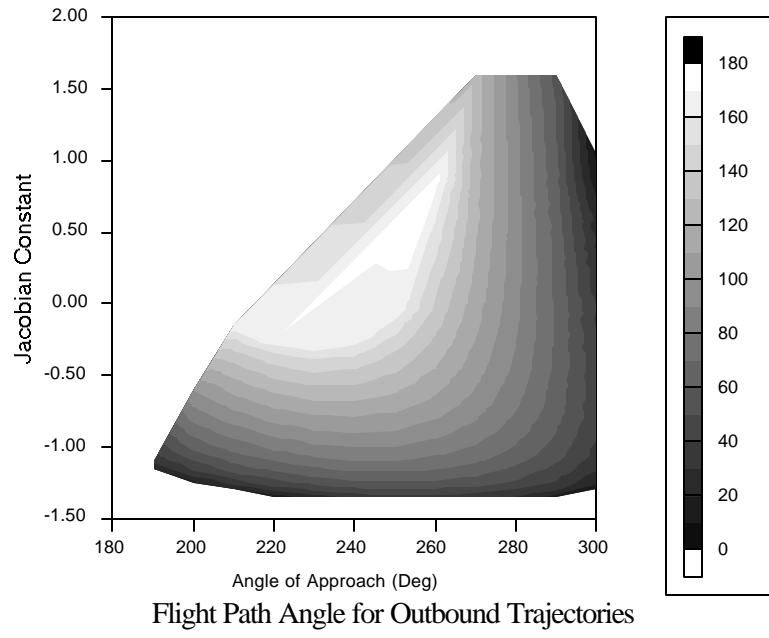


Fig. 5 – Results for the case  $R_p = 1.1 R_J$ .

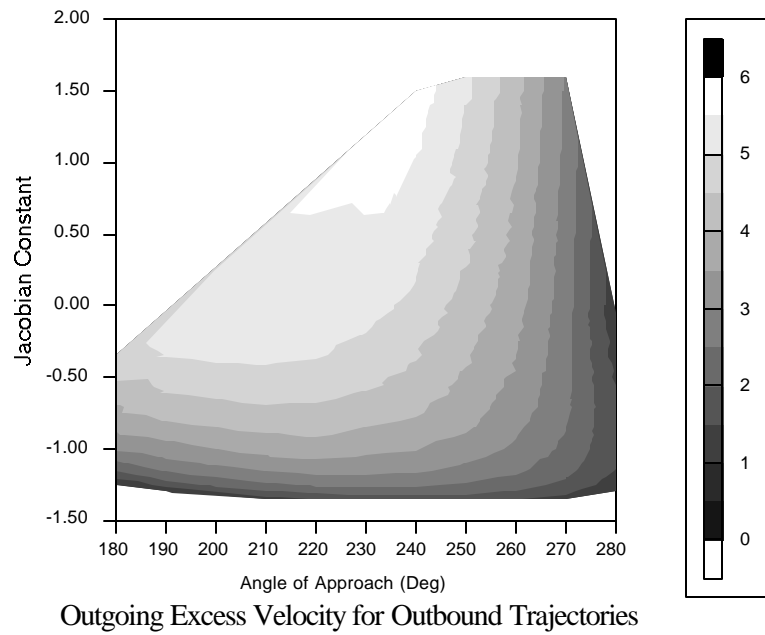
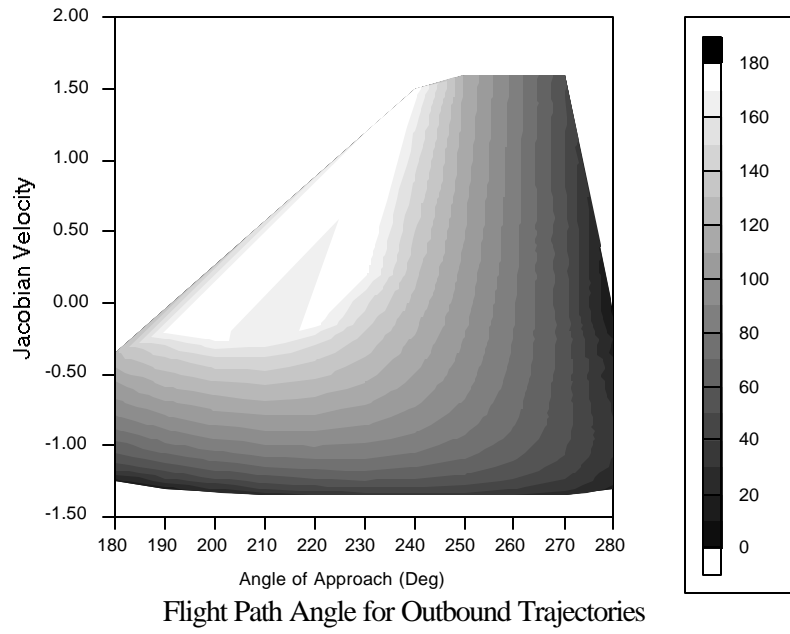
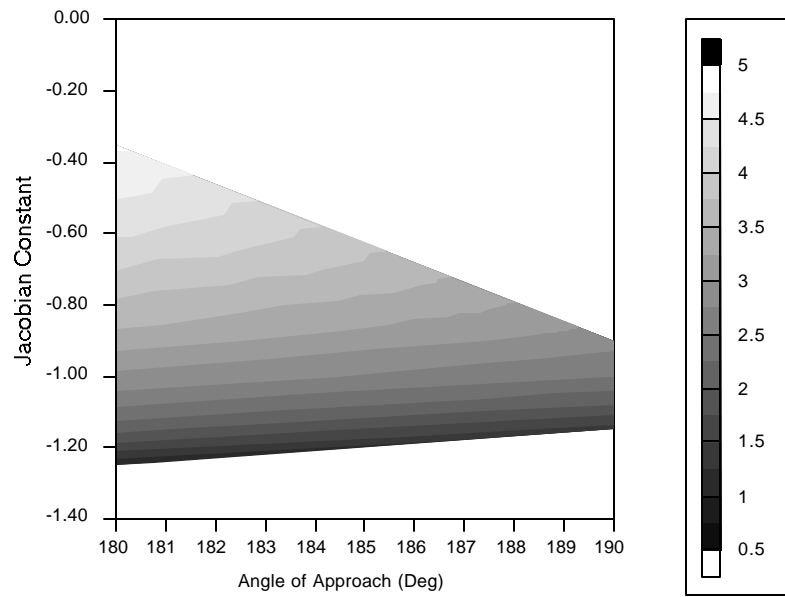
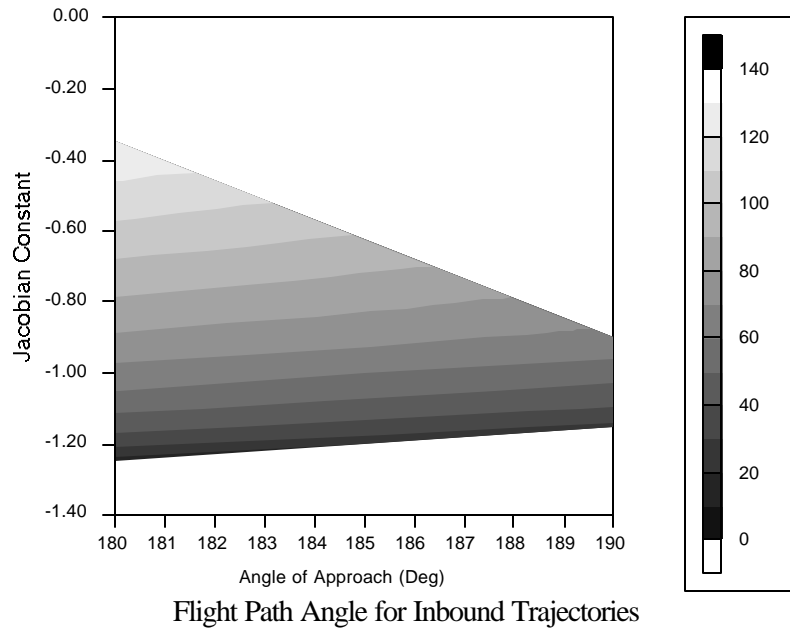


Fig. 6 - Results for the case  $R_p = 5.0 R_J$ .



Incoming Excess Velocity for Inbound Trajectories

Fig. 6 (cont.) - Results for the case  $R_p = 5.0 R_J$ .

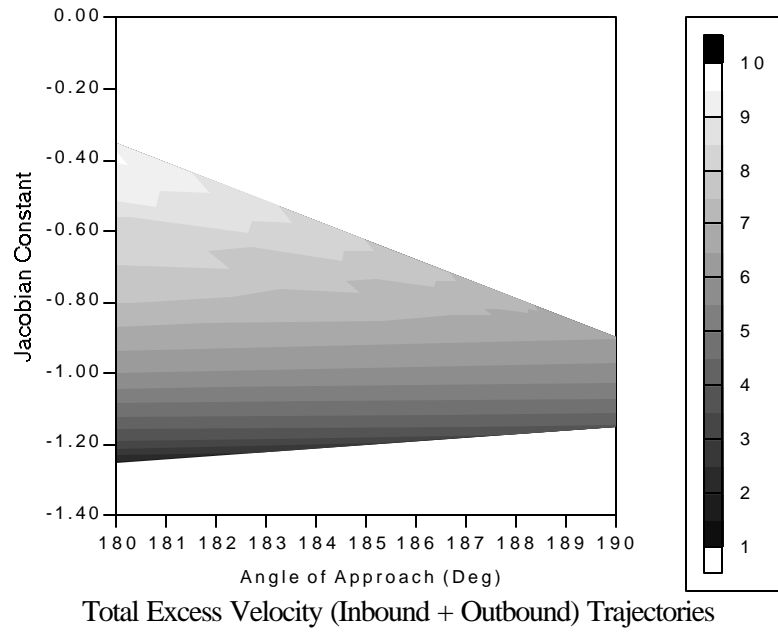


Fig. 6 (cont.) - Results for the case  $R_p = 5.0 R_J$ .

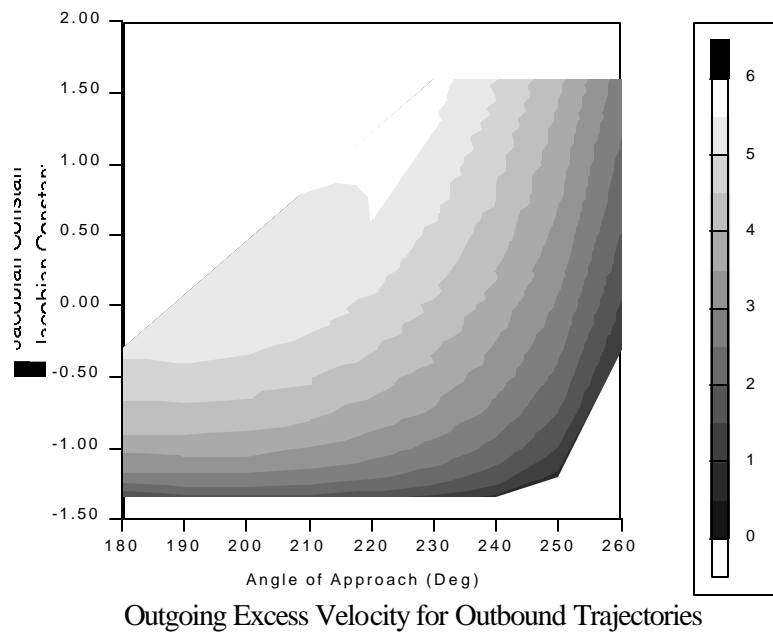
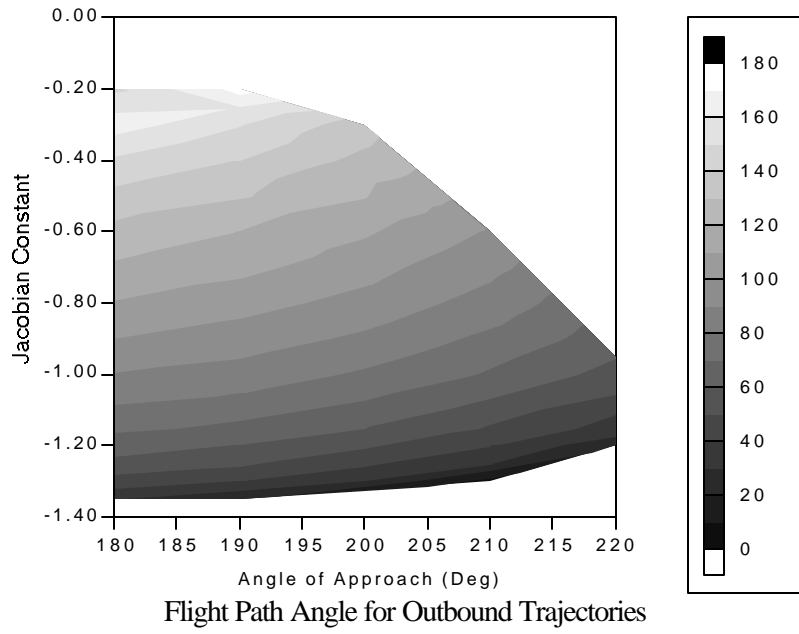
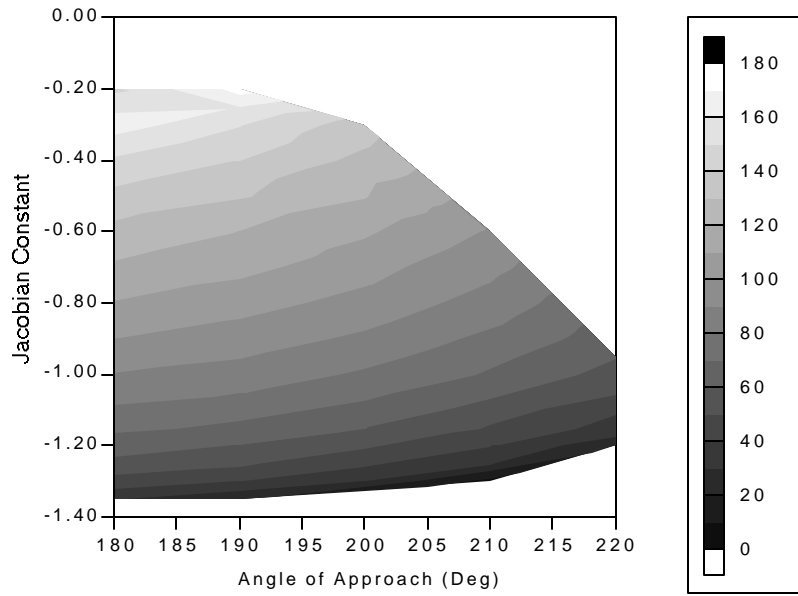
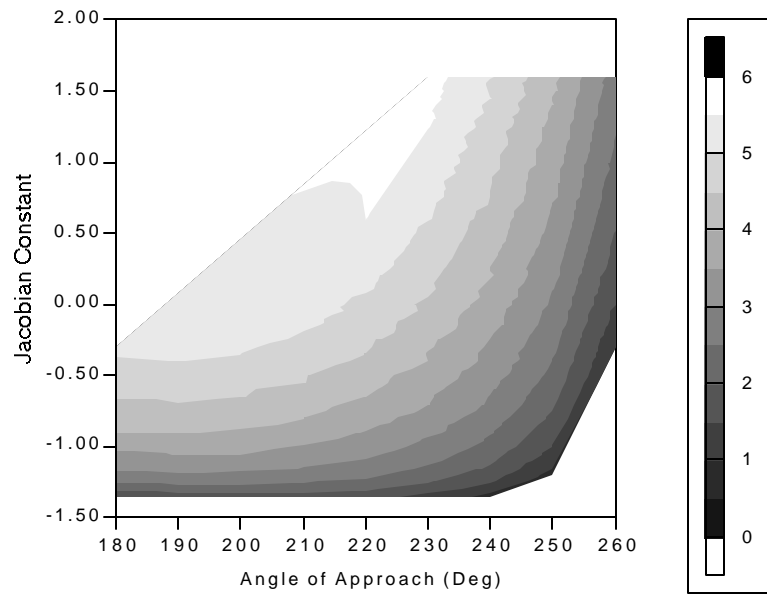


Fig. 7 - Results for the case  $R_p = 50.0 R_J$ .



Flight Path Angle for Inbound Trajectories



Incoming Excess Velocity for Inbound Trajectories

Fig. 7 (cont.) - Results for the case  $R_p = 50.0 R_J$ .

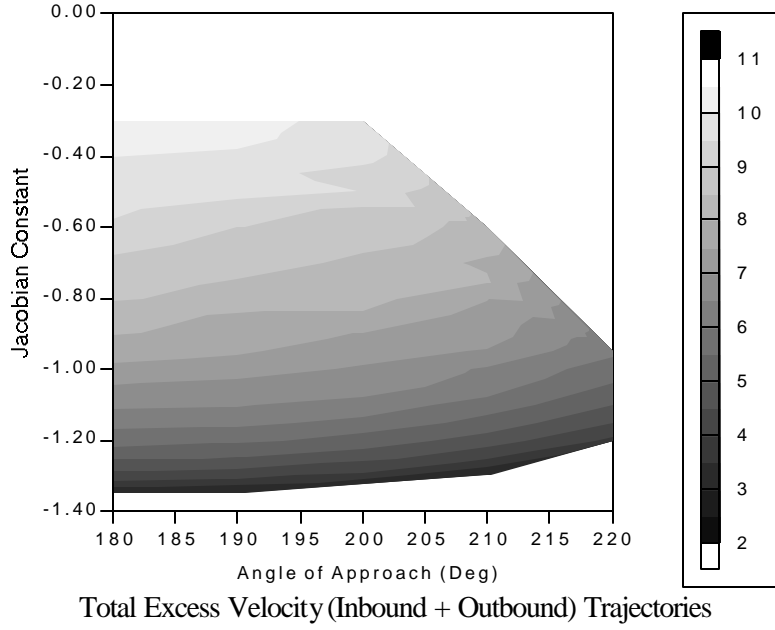


Fig. 7 (cont.) - Results for the case  $R_p = 50.0 R_J$ .

### THE “PATCHED-CONICS” APPROACH

In this section a comparison between the results obtained using the restricted problem and the “patched-conics” approximation is made. To perform this task, the following procedure is used:

i) Using the values of the energy ( $E$ -) and angular momentum ( $C$ -) before the close approach obtained by the numerical integration of the restricted problem, the semi-major axis ( $a$ ) and the eccentricity ( $e$ ) of the keplerian orbit before the passage is

obtained by  $a = -\frac{\mathbf{m}}{2E}$  and  $e = \sqrt{1 - \frac{C^2}{\mathbf{m}a}}$ . Those values are assumed to be the initial

values for both maneuvers, the one using the “patched-conics” model and the one using the restricted model;

ii) Starting from this orbit, the variation in energy and angular momentum given by the “patched-conics” model is obtained by:

$$\mathbf{DE} = \mathbf{wDC} = -2V_2V_\infty \left( \frac{1}{1 + \frac{R_p V_\infty^2}{\mathbf{m}_2}} \right) \sin(\mathbf{Y}), \text{ where } \mathbf{w} \text{ is the angular velocity of}$$

the two primaries,  $V_2$  is the velocity of the secondary body in the inertial frame and  $\mathbf{m}$  is the gravitational parameter of the secondary body ( $\mathbf{m} = Gm_2$ , where  $G$  is the universal gravitational constant);

iii) Then, the energy after the passage is obtained by  $E_{+PC} = E + \mathbf{DE}$ , as well as the angular momentum  $C_{+PC} = C + \mathbf{DC}$ ;



iv) The semi-major axis and the eccentricity of the keplerian orbit that follows the passage using the “patched-conics” model is obtained, as well as the same quantities

based in the restricted problem, using the equations  $a = -\frac{\mathbf{m}}{2E}$  and  $e = \sqrt{1 - \frac{C^2}{\mathbf{m}}}$ ;

v) Finally the variations of all the variables involved are calculated.

Figs. 8 to 10 show some of the results obtained: the difference in the variation in energy, between the two models, for the cases where  $R_p = 1.1, 5.0, 50.0 R_j$ , respectively. The difference between the two models is defined as (Variation in energy calculated by the “patched-conics” model) - (Variation in energy calculated by the restricted problem), so positive values means that the “patched-conics” model gives a higher value for the variation in energy. The velocity of approach is used as an independent variable to replace the Jacobian constant, because this constant does not exist in the “patched-conics” approximation. The results showed that the differences between the two models:

- decrease in magnitude when the periapsis distance increase, what is expected since the general effects of the swing-by decrease with this variable;
- the most negative values for this variable are concentrated close to  $\mathbf{Y} = 270^\circ$  for the smallest values of the velocity of approach, so the “patched-conics” model underestimated the variation in energy close to the maximum effect of the Swing-By;
- the most positive values for this variable are concentrated in the interval  $1.5 < V_\infty < 2.0$  and  $210^\circ < \mathbf{Y} < 240^\circ$ ;
- the typical values for the energy variation have an order of magnitude 1.0, so the maximum differences between the two models (about 0.05) are in the order of 5 %. A detailed plot with the differences expressed in percentage is not shown, because values of the variation in energy close to zero generate values too large for the percentage error;
- the influence of those differences in the semi-major axis, eccentricity and angular momentum before and after the passage were also studied. The detailed results are not shown here due to the limitation of space, but they are of the same order of magnitude,

except for situations where the energy is small. In those cases, since  $a = -\frac{\mathbf{m}}{2E}$ , small

alterations of the variation in energy causes a large variation in the semi-major axis, eccentricity and angular momentum of the orbits involved and in the excess velocity and flight path angle in the crossing points with the Earth’s orbit. A detailed study for the case  $R_p = 1.1 R_j$  showed that trajectories with energy before or after the passage small enough to cause an error in the semi-major axis greater than 0.1 canonical units (10% of the Sun-Jupiter distance) occur in 5% of the trajectories calculated. There are also trajectories with errors in semi-major axis of several hundreds of canonical units. In those situations, the use of more complex models, like the one shown here is justified.

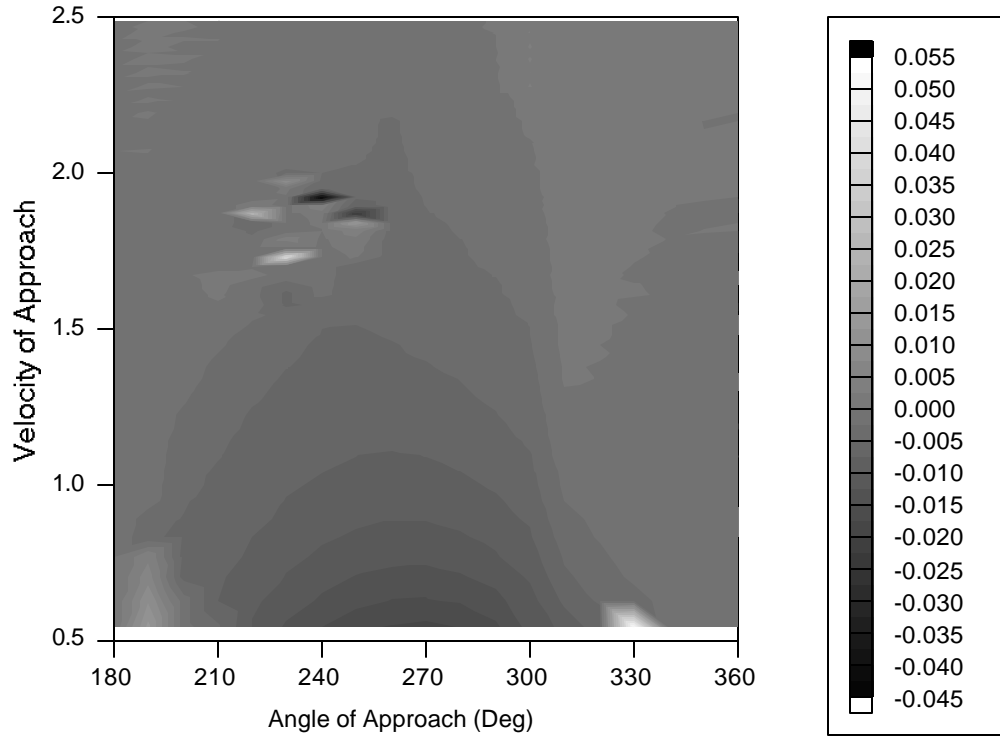


Fig. 8 – Difference of the variation in energy between the two models for  $R_p = 1.1 R_j$ .

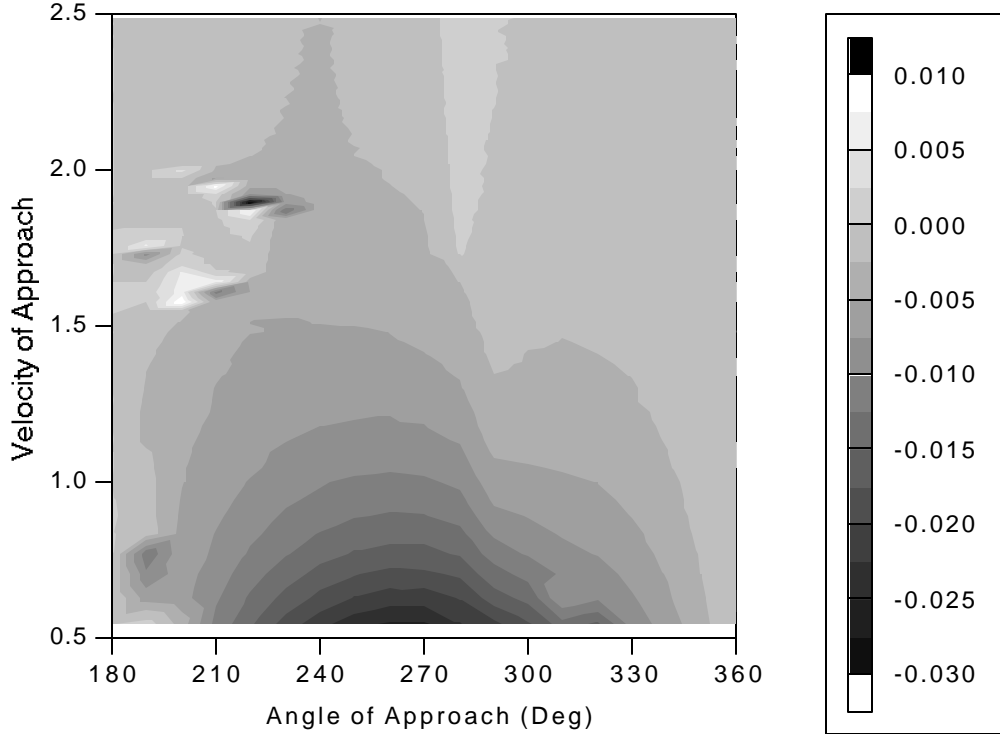


Fig. 9 – Difference of the variation in energy between the two models for  $R_p = 5.0 R_j$ .

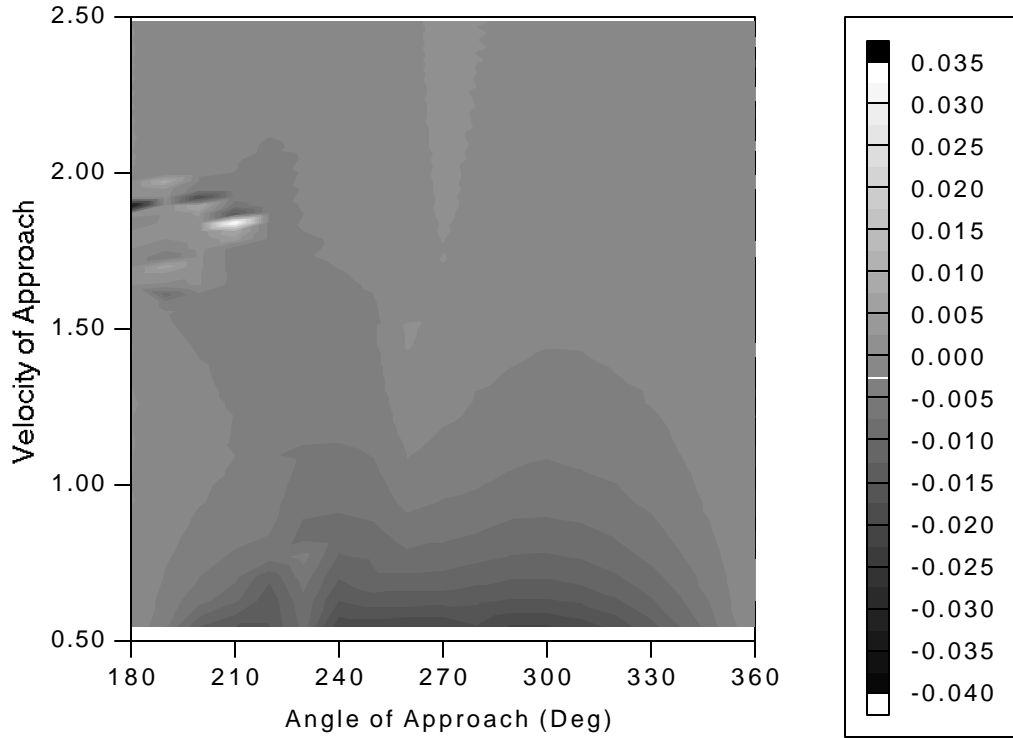


Fig. 10 – Difference of the variation in energy between the two models for  $R_p = 50.0 R_J$ .

## CONCLUSIONS

A numerical algorithm to calculate the effects of a close approach with Jupiter in the trajectory of a spacecraft is developed. Many trajectories are classified and some of them are shown in detail. It is also shown which ones of those trajectories have a potential use for missions involving departures from the Earth or returns to the Earth. The theoretical prediction that for  $0^\circ \leq \gamma \leq 180^\circ$  the spacecraft losses energy and for  $180^\circ \leq \gamma \leq 360^\circ$  the spacecraft gains energy is confirmed.

The outgoing and the incoming excess velocities of the spacecraft with respect to the Earth involved in those transfers are calculated, as well as the flight path angles at the point where the orbits of the spacecraft and the Earth intersect. Those results are sufficient to identify regions of minimum excess velocities for practical maneuvers.

After that, a procedure was developed to study the differences in the effects of the close approach predicted by the two models studied for the dynamics. The results showed that there is a good agreement of the results in the majority of the situations, but there are large discrepancies when the energy before or after the passage is small. In about 5% of the trajectories simulated the differences in semi-major axis predicted by the two models were larger than 10% of the Sun-Jupiter distance. Trajectories with differences in the order of several hundreds of Sun-Jupiter distances were also encountered. Those trajectories are the main reason to use more complex models to study this problem. In terms of energy change, the largest discrepancies obtained were about 5%.

A good strategy is to use the “patched-conics” approximation for a first study, including the study of timing conditions for the encounter with the Earth, and after that to use the restricted problem model to improve the accuracy of the results and verify if a situation of small energy does occur.

## REFERENCES

- Broucke, R. A., 1988, "The Celestial Mechanics of Gravity Assist". AIAA paper 88-4220. In: AIAA/AAS Astrodynamics Conference, Minneapolis, MN, 15-17 Aug. 1988.
- . Broucke, R.A. and Prado, A.F.B.A., 1993, "Jupiter Swing-By Trajectories Passing Near the Earth," *Advances in the Astronautical Sciences*, Vol. 82, No II, pp. 1159-1176.
- Dowling, R. L.; Kosmann, W. J.; Minovitch, M. A.; Ridenoure, R. W., 1991, "Gravity Propulsion Research at UCLA and JPL, 1962-1964". In: 41<sup>st</sup> Congress of the International Astronautical Federation, Dresden, GDR, 6-12 Oct. 1991.
- Dunham, D.; Davis, S., 1985, "Optimization of a Multiple Lunar-Swingby Trajectory Sequence". *Journal of Astronautical Sciences*, Vol. 33, No. 3, pp. 275-288.
- Farquhar, R. W. and Dunham, D. W., 1981, "A New Trajectory Concept for Exploring the Earth's Geomagnetic Tail", *Journal of Guidance, Control and Dynamics*, Vol. 4, No. 2, pp 192-196.
- Farquhar, R.; Muhonen, D.; Church, L. C., 1985, "Trajectories and Orbital Maneuvers for the ISEE-3/ICE Comet Mission". *Journal of Astronautical Sciences*, Vol. 33, No. 3, pp. 235-254, July-Sept. 1985.
- Flandro, G., 1966, "Fast Reconnaissance Missions to the Outer Solar System Utilizing Energy Derived from the Gravitational Field of Jupiter". *Astronautical Acta*, Vol. 12, No. 4.
- Minovich, M. A., 1961, "A Method for Determining Interplanetary Free-Fall Reconnaissance Trajectories", JPL Tec. Memo 312-130, Aug. 23 1961, 47 pp.
- Prado, A. F. B. A., 1996, "Powered Swing-By". *Journal of Guidance, Control and Dynamics*, Vol. 19, No. 5, pp. 1142-1147.
- Prado, A. F. B. A., 1997, "Close-Approach Trajectories in the Elliptic Restricted Problem". *Journal of Guidance, Control and Dynamics*, Vol. 20, No. 4, pp. 797-802.
- Prado, A. F. B. A., 1999, "Delta-V Estimate for Jupiter Swing-By Trajectories", *Applied Mechanics in the Americas*, Vol. 6, 1999, pp. 263-266.
- Prado, A. F. B. A. and Broucke, R. A., 1995a, "A Classification of Swing-By Trajectories using the Moon". *Applied Mechanics Reviews*, Vol. 48, No. 11, Part 2, pp. 138-142.
- Prado, A. F. B. A. and Broucke, R. A., 1995b, "Effects of Atmospheric Drag in Swing-By Trajectory". *Acta Astronautica*, Vol. 36, No. 6, pp. 285-290.
- Swenson, B. L., 1992, "Neptune Atmospheric Probe Mission". AIAA paper 92-4371. In: AIAA7AAS Astrodynamics Conference, Hilton Head, SC, Aug. 10-12, 1992.
- Weinstein, S. S., 1992, "Pluto Flyby Mission Design Concepts for Very Small and Moderate Spacecraft". AIAA paper 92-4372. In: AIAA/AAS Astrodynamics Conference, Hilton Head, SC, Aug. 10-12, 1992.